Available online at www.sciencedirect.com
SCIENCE DIRECT®
Journal of Nuclear Materials 335 (2004) 353–358
journal of nuclear materials
www.elsevier.com/locate/jnucmat

Tritium management in the first-wall materials of A-DC and TAURO blankets

G.A. Esteban [a,*], A. Perujo [b], F. Legarda [a]

[a] UPV-EHU, Department of Nuclear Engineering and Fluid Mechanics/ESI, 48013 Bilbao, Spain
[b] Joint Research Centre, Institute for Environment and Sustainability, 21020 Ispra (VA), Italy

Received 27 April 2004; accepted 6 July 2004

Abstract

The tritium management in the first wall of two European breeding blanket options, A-DC and TAURO, has been simulated numerically to analyse the influence of the material selected: ODS–RAFM steel for the Advanced Dual-Coolant (A-DC) and SiC_f/SiC composite for TAURO options. The SRIM code has been used to simulate triton implantation and define the tritium source in each kind of material as a function of the depth. The TMAP4 code was used to analyse the posterior transitory gas transport process within the material, while taking into account the tritium transport properties of each material and the temperature variation through material thickness and operating time. Both the transient evolution and the final steady-state tritium transport behaviour have been characterised. The tritium transient flux to the coolant, the recycling flux and the absorbed tritium transient inventories have been simulated. Main conclusions have been drawn about the tritium performance of each first wall.

1. Introduction

An analysis of the tritium management is compulsory when studying the viability of any type of fusion reactors. The feasibility studies of any fusion power plant concept in respect of the blanket focus on tritium breeding, safety and environmental requirements, besides shielding and resistance to neutron irradiation. Therefore, a description of the total transient quantities of tritium absorbed by the material of the fusion reactor components and the transient fluxes to the coolant region and recycled to the plasma, is essential when evaluating the viability of a specific tritium-breeding blanket associated to any power plant concept. These factors have been taken into account in the design of the inner deuterium/tritium fuel cycle of ITER [1].

With the proposal of more advanced and efficient systems for a DEMO/PROTOTYPE reactor, integrating a complete tritium breeding blanket with future new materials and engineering techniques, the tritium management should be a general issue to be accounted for beforehand. In the European Fusion Programme, the Power Plant Conceptual Study (PPCS) has analysed four power plant models; each one based on a breeding blanket design [2]: Water-Cooled Lithium Lead (WCLL), Helium-Cooled Pebble Bed (HCPB), Advanced Dual-Coolant (A-DC) and self-cooled Pb-17Li (TAURO). The two self-cooled Pb-17Li blankets corresponding to the most advanced plant models, i.e. A-DC [3] and TAURO [4,5] show the highest technological

* Corresponding author. Tel.: +34 94 601 4272; fax: +34 94 601 4159.
E-mail address: inpesalg@bi.ehu.es (G.A. Esteban).

0022-3115/$ - see front matter © 2004 Elsevier B.V. All rights reserved.
doi:10.1016/j.jnucmat.2004.07.036

attractiveness but also demonstrate an increased associated development risk [2]. These two blankets have been selected here for the study of the tritium management within its corresponding first wall (FW). In this analysis, the tritium inventories and fluxes will be obtained for each structure and qualitative conclusions will be drawn about the performance of each FW from the tritium management point of view. Other factors affecting the tritium management within the blanket will be commented on.

2. Modelling

The tritium implantation into the FW has been estimated by a simple application of the SRIM code [6] with 300 eV monoenergetic tritons and an angle of incidence of 0°. An implanted atom flux of 3×10^{19} $m^{-2}s^{-1}$ distributed 50% between deuterium and tritium has been considered, obtaining an implantation range of 5×10^{-9} m for the steel in the case of A-DC and 7×10^{-9} m for SiC_f/SiC in the case of TAURO (Fig. 1).

The resulting implantation distributions and the surface heat fluxes together with the experimental hydrogen isotope transport properties (Figs. 2–4) and thermal properties of the FW materials (Table 1 [7–10]) have been used in the code TMAP4 [11] to model the tritium transport through the material layers of each blanket.

A 4 mm thick FW of the RAFM steel OPTIFER-IVb (similar to EUROFER) has been considered for the calculation in the case of A-DC [3], whereas a 10 mm thick FW of SiC_f/SiC composite has been simulated in the case of TAURO [4]. The primary refrigerant loop of the FW (He for A-DC and Pb-17Li for TAURO) has been modelled in TMAP4 as a layer positioned at the smallest distance from the surface facing the plasma.

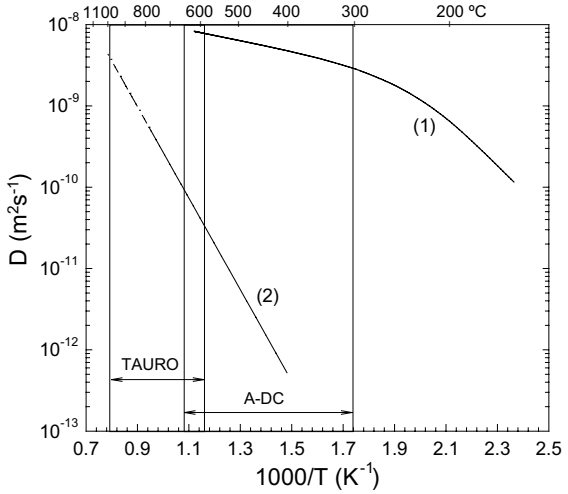

Fig. 2. Tritium diffusivities in the operation temperature range of each blanket: (1) RAFM steel [7], (2) SiC_f/SiC composite [8] (the broken line corresponds to extrapolated values).

In the case of TAURO the maximum reference value of 1300 Pa [12] has been assumed for the tritium partial pressure within the Pb-17Li breeder. The calculation time has been selected in each case to ensure that the steady state was reached. In the case of the RAFM steel the tritium diffusive transport parameters have been obtained by extrapolation from the ones experimentally estimated with hydrogen and deuterium by quantum-statistical considerations [13]. The tritium surface rate constants have been extrapolated with the classical relationship (i.e., the transport parameter inversely proportional to the square root of the atomic mass of the corresponding hydrogen isotope) because only the experimental values corresponding to one hydrogen

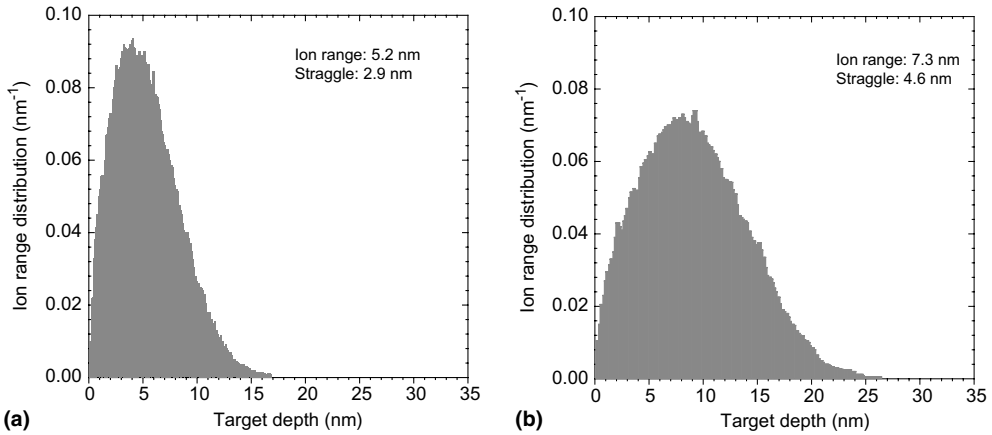

Fig. 1. Implantation distributions of tritium in the first wall of the two blankets (results from SRIM code [6]): (a) A-DC and (b) TAURO.

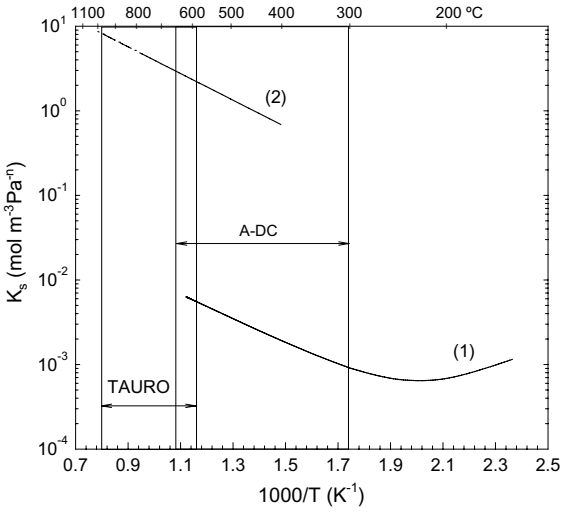

Fig. 3. Tritium Sieverts constant in the operation temperature range of each blanket: (1) RAFM steel ($n = 0.5$) [7], (2) SiC_f/SiC composite ($n = 0.22$) [8] (the broken line corresponds to extrapolated values).

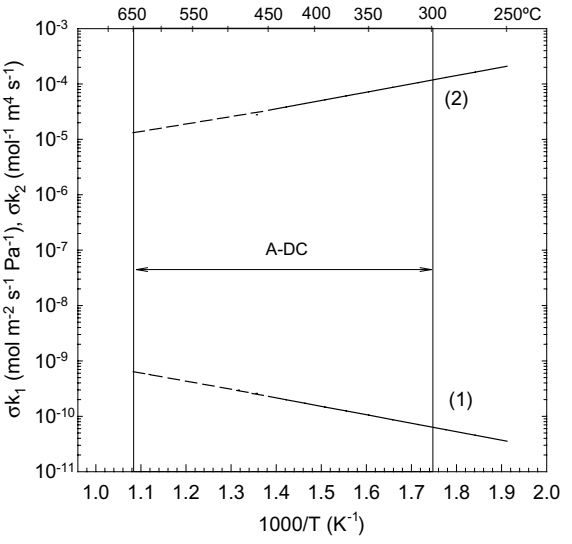

Fig. 4. Tritium adsorption (1) and recombination (2) rate constants for RAFM steel (natural oxide) [9].

isotope (deuterium) were available [9]. For the SiC_f/SiC case the classical isotopic mass relationship has been used to obtain the tritium diffusivity from the deuterium one because of the same reason. Because the data collection of SiC_f/SiC are the effective parameters of the material with the porosity included no modelling of the porosity or differentiation of the matrix and fibre phases of the material [14] is needed in the subsequent TMAP4 calculation. It is worth emphasizing that in the case of SiC_f/SiC composite a relationship between solubility and hydrogen isotopes partial pressure with a classical exponent of $n = 0.5$ is not experimentally observed, but an exponent of $n = 0.22$. The possible causes and discussion can be found in [8].

A continuous plasma operation characteristic of DEMO is supposed, quite the opposite of the pulsating operation of ITER. The calculations give the transient tritium fluxes to the primary coolant region and back to the plasma region, and the tritium inventories within the bulk of the material.

3. Results and discussion

The results of the TMAP4 evaluation in each blanket are analysed hereafter. Fig. 5 depicts the transient evolution of the tritium inventory in the A-DC blanket, whereas Fig. 6 shows the transient fluxes from the FW to the plasma (i.e. recycling flux) and to the coolant region. Figs. 7 and 8 correspond to the same variables for the TAURO blanket. A summary of the key values describing the performance of each FW is shown in Table 2.

The different time evolution for the fluxes in each blanket option is noteworthy; whereas in A-DC the steady-state permeation flux is reached in a short time (2000 s) in TAURO much longer time (3×10^5 s $\simeq$ 83 h) is needed to get that final situation. This is a predictable result considering the smaller values of tritium diffusivities in SiC_f/SiC and the range of operating temperatures of TAURO in comparison to the steel in the range of operating temperatures of A-DC (Fig. 2).

In the case of A-DC a 8% proportion of the total implanted amount of tritium permeates to the coolant. However, the behaviour of the TAURO blanket is completely different. In this case a counter-current flux from the breeding region to the plasma region has been detected.

The major part of the inventory in A-DC occupies the lattice positions rather than trapping sites. The reason for this distribution is that trapping phenomena occur in the RAFM steel at low temperatures (lower than 573 K) and in the range of the operating temperatures absorption is dominated by interstitial occupation rather than by binding to the defects of the material. Lattice and trapping inventories in TAURO have not been differentiated because such behaviour has not been experimentally accounted for in SiC_f/SiC [8].

The total amount of tritium dissolved in steady-state permeation is higher in TAURO than in A-DC, which is reasonable taking into account the Sieverts constants of tritium in SiC_f/SiC and the steel in the temperature ranges of TAURO and A-DC, respectively (Fig. 3).

The counter-current flux from the breeding region of TAURO to the plasma region presents the positive

Table 1
Tritium transport parameters and thermal properties of the RAFM steel OPTIFER-IVb and SiC_f/SiC composite [7–10]

Material	K_{s0} ($mol\,m^{-3}\,Pa^{-n}$)	E_s	D_0 ($m^2\,s^{-1}$)	E_d	N_t (sites m^{-3})	E_t	σk_{10} ($mol\,m^{-2}\,s^{-1}\,Pa^{-1}$)	E_1	σk_{20} ($mol^{-1}\,m^4\,s^{-1}$)	E_2
OPTIFER-IVb	0.271	27.9	4.17×10^{-8}	12.0	7.910^{23}	55.5	2.448×10^{-8}	29.3	2.317×10^{-7}	−28.7
SiC_f/SiC	1.5×10^{2}	30.2	0.9×10^{-4}	107.7	–	–	–	–	–	–
	Thermal conductivity (W/m K)				Specific heat capacity (J/K kg)					
RAFM steel (F82H)	$28.384-0.011777T-1.0632\times10^{-6}T^2-8.2935\times10^{-9}T^3$				$1390.2-7.8498T+0.022969T^2-2.7446\times10^{-5}T^3+1.1932\times10^{-8}T^4$					
SiC_f/SiC	15				1100					

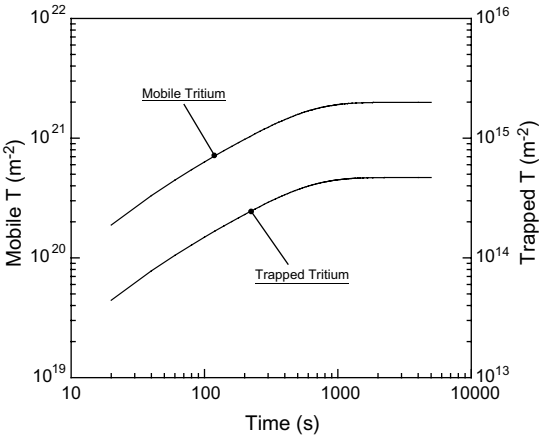

Fig. 5. Mobile and trapped tritium inventories evolution within the FW of A-DC blanket.

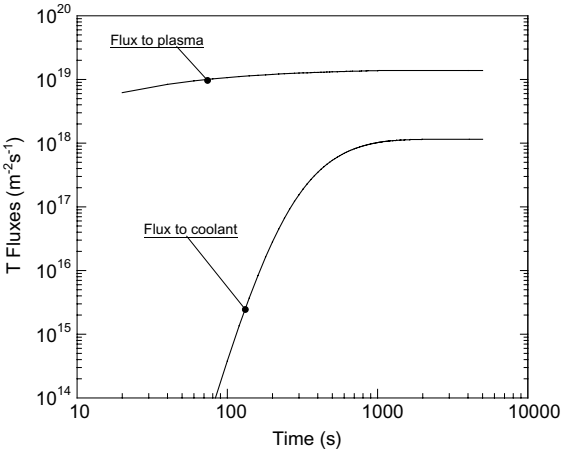

Fig. 6. Tritium fluxes to plasma and primary coolant loop in A-DC blanket.

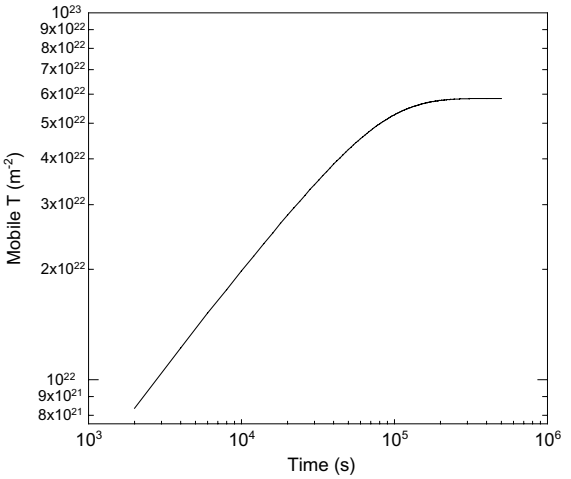

Fig. 7. Mobile tritium inventory evolution within the FW of TAURO blanket.

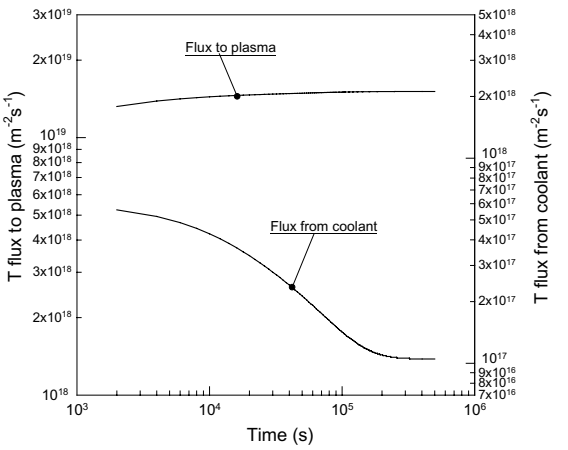

Fig. 8. Tritium fluxes to plasma and from primary coolant loop in TAURO blanket.

aspect of direct recuperation of the bred tritium into the plasma and a subsequent reduction of the technological requirements in the tritium recuperation systems operating outside the blanket. Furthermore, the thermally recycled H isotopes may impinge on and cool the plasma

Table 2
Tritium management key values for each blanket first wall: tritium inventories and fluxes in steady state, and transient progress evaluation

Blanket	Interstitial (tritium m^{-3})	Trapping (tritium m^{-3})	Recycling (tritium $m^{-2}s^{-1}$)	Flux to the coolant region (tritium $m^{-2}s^{-1}$)	Operating time to reach steady state operation
A-DC	2.0×10^{21}	4.7×10^{14}	1.38×10^{19}	1.15×10^{18}	2000 s
TAURO	5.8×10^{22}	–	1.5×10^{19}	-1.1×10^{17}	83 h

edge; the resulting necessity of particle balance adjustment should be borne in mind as well. This bred tritium permeation from the coolant-breeding region to the plasma is similar to the case explained in [15], wherein hydrogen from the FW water coolant loop was added to prevent corrosive effects of radiolysis permeated into the vacuum vessel.

The objective of this study is restricted to the influence of the type of FW material (i.e., its tritium transport properties and thermal properties) on the tritium management of any blanket. Other factors influencing the hydrogen isotopes transport have not been included so as not to complicate excessively the transient numerical calculation or they are not fully known or described completely at the moment; these additional factors are identified and qualitatively analysed henceforth.

Thermo migration (Soret effect) through the material has not been considered, i.e., the hydrogen isotope migration induced by the temperature gradient through the width of the FW. This process depends on the Ludwig–Soret thermodiffusion heat Q^*, which has not been evaluated yet for the materials SiC_f/SiC and OPTIFER-IVb treated here.

In relation to the A-DC blanket option, the H isotope bulk transport properties of the ODS-EUROFER material should approximate, though it is not exactly the same as the properties of the RAFM steel OPTIFER-IVb considered here. Similar hydrogen isotopes diffusive transport properties have been reported for various RAFM steels [7] with the same basic microstructure of the lattice (i.e. bcc). Moreover, surface rate constants are expected to vary because of the particular surface state (nano-structured layer of yttrium oxide). Here the assumption of a perfect sputter-cleaned surface may not be considered because the stable permanent nano-structured oxide is formed on the steel expressly in order to prevent the sputtering. The oxide dispersion strength layer could impede the dissolved H isotopes re-emission to the plasma because of a substantial reduction in the recombination coefficient and provoke a certain forced flux to the cooling He region. The effect of oxide layer on H transport in metals is well known as an inhibitor of the surface processes of adsorption and desorption [16]. The particular transport properties of H isotopes through this specific material should be analysed in future experiments; in the mean time, the assumption of the parameters coming from OPTIFER-IVb (Fig. 4) with natural oxide may represent a reasonable approximation.

In operating conditions the radiation presence should modify the H isotope transport characteristics because radiation enables induced diffusion mechanisms different from over-barrier jumping due to ground-state thermal vibration of the tritium atoms [17]. In addition, the high energy neutrons coming from fusion reactions are expected to induce the amorphisation of silicon carbide and additional defects in the steel, which should lead to effective trapping sites for additional tritium accumulation. Ion-generated defects in the first layer may influence in the trapping inventory too, though they hold less significance than neutron-generated defects. Nevertheless, the trapping phenomena should not have any influence on the steady-state permeation flux values; only the time necessary to reach the steady state should be increased with creation of new trapping sites. Another effect to be taken into account is the variation of the effective FW thickness provoked by sputtering erosion of the wall and surface deposition of material coming from other regions of the blanket.

The high impinging fluxes may create a saturation state of the H species on the FW, which leads to H bubble nucleation and recycling enhancement of the H excess that cannot occupy dissolution interstitial positions.

In the present evaluation, a tritium implanted flux of 3×10^{19} $m^{-2}s^{-1}$ has been considered as a reference value. This value may undergo high variation when going through the poloidal coordinate in the blanket, showing higher values the closer the divertor region is. This fact should not disturb the relative tritium transport kinetics; though, the final inventory and flux values would be escalated in the same proportion as the implanted flux. The simplification of the SRIM calculation has no influence in the preposterous TMAP4 routine because any relative variation in the nanometrical scale is negligible in comparison to the diffusion path length magnitude (millimetres). Only the recycling values might undertake a slight variation in the time scale. In addition, other factors such as sputtering, codeposition or the surface roughness may mask that possible deviation.

In the one-dimensional TMAP4 calculation, the assumption of the coolant being a layer after the FW may produce an overestimation of the interphase surface

area in the case of A-DC because the real situation corresponds to a series of He cooling tubes. This fact may provoke a quantitative overestimation of the tritium permeation flux. That is not the case of the TAURO blanket because the corresponding FW is cooled by a layer of liquid Pb-17Li flowing through a curved rectangular channel that covers a spread area of FW rather than individual cooling tubes.

In the case of TAURO, a possible improvement in the calculation could be performed by evaluating the tritium concentration and partial pressure distribution in the breeding liquid Pb-17Li as a function of the flowing circuit length instead of considering an average constant value. In the case of A-DC, the coupling of the secondary bred tritium coming from the Pb-17Li loop through the SiC_f/SiC flow channel inserts will improve the evaluation of tritium inventories and fluxes. A final interesting question for future analysis would be a more complicated three-dimensional non-steady state calculation to study the geometrical particularities of each blanket, instead of the one-dimensional scheme proposed in TMAP 4.

4. Conclusions

An exploratory study has been performed on the influence of the material selected for the construction of the first wall in the tritium management within that part of a breeding blanket. Two blanket concepts, A-DC and TAURO, have been selected to analyse the differences in the tritium behaviour coming from the first-wall material used in each case. The type of material and its associated tritium transport properties have resulted to be determinant in the operation of each first wall from the tritium management point of view.

The steady-state tritium flux to the coolant is significant in the case of A-DC and its transitory evolution is fast due to high values of diffusivity of tritium in the RAFM and a low recombination constant of the plasma facing surface; a special care should be taken of the detritiation systems of the helium loop. Because of the high operating temperatures a low tritium inventory (seven orders of magnitude lower than the inventory dissolved in interstitials) is trapped in microstructural defects of the material. An 8% fraction of the implanted tritium releases into the helium-cooled loop, the rest being recycled into the plasma. In comparison to A-DC, the TAURO blanket design has shown a higher steady-state tritium inventory reached by less than four operation days because of the high tritium solubility in SiC_f/SiC. Additionally, the fact that the coolant region is simultaneously a tritium breeding region provokes a counter current flux of the bred tritium to the plasma region, assuring a natural tritium recovering and a relaxation of the design requirements imposed to external tritium recovering systems.

The dependence of the tritium management on the type of FW material selected has been demonstrated. A broad tritium analysis of every blanket and divertor option by applying a three-dimensional non-steady-state calculation to the respective material layered configuration is highly desired in order to evaluate the respective tritium management feasibility.

References

[1] M. Glugla, R. Lässer, L. Dörr, D.K. Murdoch, R. Haange, H. Yoshida, Fusion Eng. Des. 69 (2003) 39.
[2] G. Marabach, I. Cook, D. Maisonnier, Fusion Eng. Des. 63&64 (2002) 1.
[3] P. Norajitra, L. Bühler, U. Fischer, K. Kleefeldt, S. Malang, G. Reimann, H. Schnauder, L. Giancarli, H. Golfier, Y. Poitevin, J.F. Salavy, Fusion Eng. Des. 58&59 (2001) 629.
[4] L. Giancarli, J.P. Bonal, A. Caso, G. Le Marois, N.B. Morley, J.F. Salavy, Fusion Eng. Des. 41 (1998) 165.
[5] H. Golfier, G. Aiello, M. Fütterer, L. Giancarli, A. Li-Puma, Y. Poitevin, J. Szczepanski, Fusion Eng. Des. 61&62 (2002) 461.
[6] J.F. Ziegler, SRIM, The Stopping and Range of Ions in Matter, Instruction Manual, IBM Research, Yorktown, New York, 2003.
[7] G.A. Esteban, A. Perujo, K. Douglas, L.A. Sedano, J. Nucl. Mater. 281 (2000) 34.
[8] G.A. Esteban, A. Perujo, F. Legarda, L.A. Sedano, B. Riccardi, J. Nucl. Mater. 307–311 (2002) 1430.
[9] G.A. Esteban, A. Perujo, L.A. Sedano, B. Mancinelli, J. Nucl. Mater. 282 (2000) 89.
[10] A.A. Tavassoli, J.W. Rensman, M. Schirra, K. Shiba, Fusion Eng. Des. 61&62 (2002) 617.
[11] G.R. Longhurst, D.F. Holland, J.L. Jones, B.J. Merrill, TMAP4 User's Manual, Idaho National Engineering Laboratory EGG-FSP-10315 (1992).
[12] L. Giancarli, M.A. Fütterer, Water-cooled Pb-17Li DEMO blanket line status report on the related EU activities, CEA report, DMT 95-505/SERMA/LCA/1801 (1995).
[13] G.A. Esteban, F. Legarda, L.A. Sedano, A. Perujo, Fusion Sci. Technol. 41 (2002) 948.
[14] G.A. Esteban, A. Perujo, F. Legarda, L.A. Sedano, B. Riccardi, Fusion Eng. Des. 69 (2003) 463.
[15] O.V. Ogorodnikova, M.A. Fütterer, E. Serra, G. Benamati, J.F. Salavy, G. Aiello, J. Nucl. Mater. 273 (1999) 66.
[16] G.A. Esteban, A. Perujo, L.A. Sedano, F. Legarda, B. Mancinelli, K. Douglas, J. Nucl. Mater. 300 (2002) 1.
[17] L. Sedano, A. Perujo, B.G. Polosukhin, N.G. Primakov, I.L. Tazhibaeva, in: C. Varandas, F. Serra (Eds.), Fusion Technol. 1996, Proceedings of the 19th SOFT, Lisbon, 1996 (1997) 1415.